34th Annual International Conference of the IEEE EMBS
San Diego, California USA, 28 August - 1 September, 2012

Evaluation of an image-based tracking workflow using a passive marker and resonant micro-coil fiducials for automatic image plane alignment in interventional MRI

M. Neumann[1,3], E. Breton[1], L. Cuvillon[1], L. Pan[2], C.H. Lorenz[2], M. de Mathelin[1]

Abstract— **In this paper, an original workflow is presented for MR image plane alignment based on tracking in real-time MR images. A test device consisting of two resonant micro-coils and a passive marker is proposed for detection using image-based algorithms. Micro-coils allow for automated initialization of the object detection in dedicated low flip angle projection images; then the passive marker is tracked in clinical real-time MR images, with alternation between two oblique orthogonal image planes along the test device axis; in case the passive marker is lost in real-time images, the workflow is reinitialized. The proposed workflow was designed to minimize dedicated acquisition time to a single dedicated acquisition in the ideal case (no reinitialization required). First experiments have shown promising results for test-device tracking precision, with a mean position error of 0.79 mm and a mean orientation error of 0.24°.**

I. INTRODUCTION

INTERVENTIONAL magnetic resonance imaging (MRI) is gaining interest for real-time monitoring of percutaneous procedures, such as ablations of tumors, biopsies and infiltrations. Its advantages over interventional computer tomography (CT) include absence of radiation exposure for both patient and medical staff, better soft tissue contrast and free image plane orientation and positioning. Nevertheless, manual alignment of the image planes to the interventional tool is a time-consuming task requiring trained MR technologists. Several methods have been presented in the past for object detection and automatic scan plane alignment, either based on active or passive tracking devices.

On one hand, systems using active tracking devices rely on wired micro-coils [1] or optical tracking systems [2]. For approaches based on the measurement of MRI gradient fields, receiver coils are embedded in a device to determine its position and orientation without using the acquired images [1]. For active device tracking, the requirement of dedicated tracking gradients during the MRI sequence, consideration of coil heating and expensive instrumentation are inherent drawbacks to these systems, which are connected by wire to the MRI hardware.

Optical systems use cameras and markers in order to determine the orientation and position of an object inside the MRI scanner [3] [4]. However, these optical systems require both an accurate calibration and an unobstructed line-of-sight between the marker and the camera located outside of the MRI scanner.

On the other hand, systems using passive tracking devices apply MR image-based tracking approaches. In [5] the signature of a ferromagnetic object is tracked in 3D using a correlation function applied to a projection of the signal on each of the three MRI axes. Even though this method seems to overcome the following passive tracking systems in precision and acquisition time, the use of a ferromagnetic object results in high susceptibility artifacts in the image.

In [6] a stereotactic frame is used. The frame consists of acrylic plastic with seven embedded glass cylinders filled with a contrast agent. The intersection points of the glass cylinders with only one scan plane allow to determine the position and orientation of the frame. The main limit of the system is the bulkiness of the stereotactic frame. Smaller systems have been proposed based on the use of one [7] [8] or two [9] cylindrical passive markers. Two tracking image planes are then acquired orthogonally to the main axis of the marker, the intersection of the cylinder is detected in both planes in order to calculate the orientation and position of the marker. Main limitation of this approach is the need for two dedicated tracking image planes for the acquisition of a single marker-aligned image plane.

Another technique is based on the use of resonant micro-coils that are tuned to the Larmor frequency of the scanner. In low flip angle acquisition, only very small signal is received from anatomical structures, while the micro-coils are depicted as bright regions in the image. Thus detection of micro-coils can be easily achieved by intensity-based algorithms [10]. Position and orientation of a micro-coil equipped device can be computed from projections of the micro-coils' signal on 2 orthogonal scan planes [11]. However, micro-coils have the main drawback of requiring dedicated low flip angle images, that are unusable for image-guided procedures due to the lack of signal from anatomical structures.

Main advantages of most image-based tracking techniques are that they need neither expensive instrumentation nor any calibration, as markers and patients are depicted in the same images. Nevertheless, image-based tracking methods usually require user dependent manual initialization and reinitialization steps.

In this paper we evaluate the feasibility and primary results of a hybrid workflow using a detection and tracking

Manuscript received March 15, 2012.

[1]Laboratoire des Sciences de l'Image, de l'Informatique et de la Télédétection, Strasbourg, France.

[2]Center for Applied Medical Imaging, Siemens Corporate Research, Baltimore, MD, United States.

[3]Correspondence to: Markus Neumann, Laboratoire des Sciences de l'Image, de l'Informatique et de la Télédétection, 1 Place de l'Hôpital, 67091 Strasbourg (France); email: m.neumann@unistra.fr

algorithm for a passive marker and resonant micro-coil fiducials. This image-based tracking workflow is designed for fully automated image plane alignment, with minimization of tracking-dedicated time.

II. MATERIALS

A. Micro-coils

In-house micro-coils are built in a similar manner as in [4]. A total of 6 turns of 0.4 mm diameter enameled wire are wound around a 7.5 mm diameter plastic tube (Eppendorf) in order to obtain an inductance of around 300 nH and a quality factor larger than 60. A 22 pF capacitor is soldered in series to the inductance. A network analyzer is used during fine-tuning of the micro-coil resonance frequency to 63.68 MHz (Larmor frequency of the 1.5 T MRI scanner) by spreading its windings. As soon as the resonance frequency is tuned, windings are fixed with superglue. Finally, the tube is filled with a 1/100 contrast agent (Gd-DTPA 0.5 mM) dilution in water in order to obtain a signal in the MR images (Fig. 1a).

B. Passive Marker and Assembled Test Device

The passive marker is a plastic tube (length: 10.5 cm, diameter: 1.4 cm) filled with the same contrast agent solution as above (Fig. 1b). The test device is made of two resonant micro-coils rigidly fixed at the endings of the passive marker (Fig. 1c).

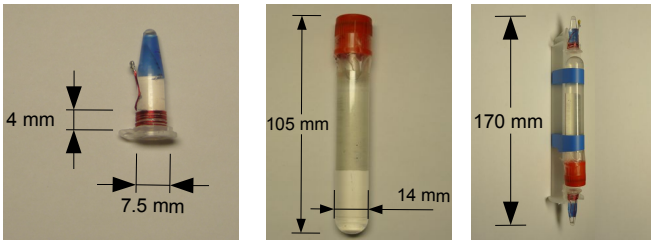

(a) (b) (c)

Fig. 1: (a) Micro-coil wound around a plastic tube that is filled with contrast agent solution. (b) Passive marker consisting of a plastic tube that is filled with the same contrast agent solution. (c) Assembled test device with 2 micro-coils at endings of the passive marker.

III. METHODS

A. MRI settings

All experiments were performed using the body coil in an open bore 1.5 T MRI scanner (MAGNETOM Aera, Siemens AG, Erlangen, Germany). An interactive, real-time, multi-slice TrueFISP sequence (Beat_IRTTT [12], Siemens Corporate Research & Technology, USA) was used for image acquisition. The passive marker is used for detection in clinical real-time images. Imaging parameters of the clinical real-time sequence include: matrix 202×224, FOV 400×400 mm^2, spatial resolution 1.79×1.79 mm^2, slice thickness 4 mm, TE 2.2 ms, TR 4.1 ms, flip angle 50°, bandwith 260 Hz/Px, temporal resolution 819 ms. The two micro-coils are used for detection in dedicated low flip angle acquisitions with the same imaging parameters except: slice thickness 100 mm and flip angle 1°. These projection images are not clinically usable by the physician.

B. Workflow

The objective of the presented workflow is to automatically control the 2 oblique image planes (transversal and sagittal) to align along the main axis of the previously described test device. This workflow was designed to minimize tracking dedicated acquisition time, i.e. use of projection images.

1) Initialization: A dedicated low flip angle transversal projection at the MRI scanner isocenter is acquired (Fig. 2a). After detection of the two micro-coils, the position and orientation of the test device is calculated. Imaging coordinates of a simple oblique sagittal plane aligned on the main axis of the test device are calculated and sent to the MRI scanner (Fig. 2b).

2) Image Plane alignment: A real-time simple oblique sagittal image is acquired with the previously calculated coordinates (Fig. 2c). The passive marker is then detected, its orientation and position are calculated and used for the definition of a double oblique transversal image plane along the main axis of the test device (Fig. 2d). A real-time image is acquired with the calculated coordinates (Fig. 2e). Detection is repeated in the transversal image plane for the definition of an updated simple oblique sagittal image plane along the main axis of the test device (Fig. 2f). This step is repeated as desired for image plane updates on current test device positions. If detection of the passive marker on one of the simple oblique image planes fails, a reinitialization of the workflow is necessary (step 3).

3) Reinitialization: This step is similar to step 1 except the dedicated transversal projection is centered at the last correctly detected position of the passive marker.

C. Image Segmentation

1) Segmentation of Micro-coils: The segmentation of the micro-coils is performed by using the phase-only cross-correlation (POCC) algorithm [13]. The normalized cross-correlation between the projection image and a self-made micro-coil search-pattern is carried out in k-space. After inverse Fourier Transform of the normalized cross-correlation, the micro-coils can be detected as local maxima.

2) Segmentation of the Passive Marker: The first step for the segmentation of the passive marker is a preliminary segmentation by thresholding in order to distinguish the image background and regions of interest (ROI). Before thresholding (Fig. 3a), a Gaussian diffusion filter is applied on the image in order to avoid over-segmentation caused by small anatomical structures inside the patient's body. An efficient threshold can be found at the local minimum after the highest pixel intensity in the histogram of the filtered image (Fig. 3b). After thresholding, morphological operations are applied on the image in order to fill the holes

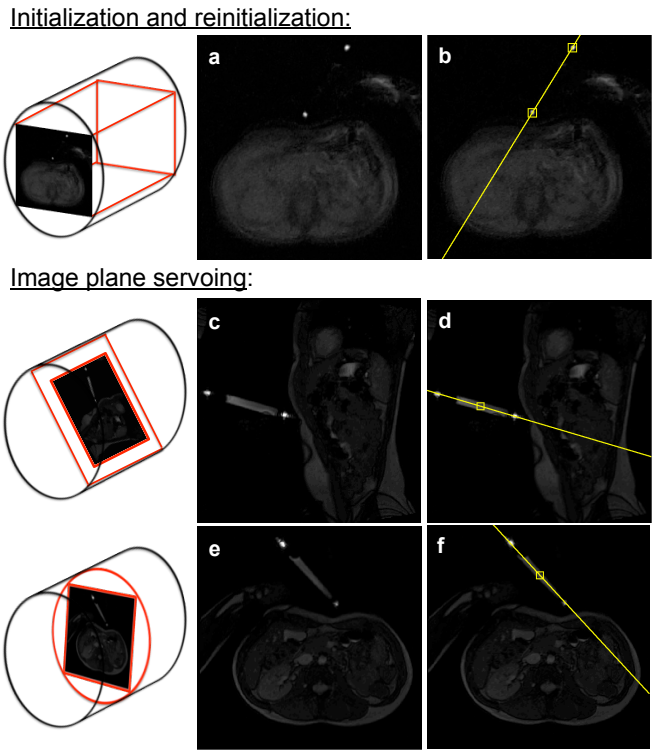

Fig. 2: Workflow with real-time and dedicated projection images and the corresponding space acquired inside the MRI scanner (left column).

in segmented objects and to separate distinct objects that have been linked due to thresholding (Fig. 3c).

The second step is to find the ROI containing the passive marker. The biggest ROI is discarded, as the biggest segmented object in the image is the patient's body. Moreover, a size criterion is applied on the rest of the ROIs in order to discard any potentially segmented micro-coil (Fig. 3d). Afterwards, the ROI containing the pixel with the highest intensity is considered to be the ROI that contains the marker. This is based on the assumption that the passive marker is filled with contrast agent that gives a very bright signal in the image. Nevertheless this assumption is not true for the original image, as the patient's body and the micro-coils are also regions of high pixel intensities. Note that signal intensity in the micro-coils can not be used for tracking in clinical images as their intensity varies a lot with imaging parameters due to high quality factor.

Third step is to segment the passive marker inside the chosen ROI. As the physician's hand that is holding the marker is also depicted in the image, parts of it can be contained in the ROI together with the marker. Once again a Gaussian diffusion filter is applied in order to avoid over-segmentation of the small anatomical structures inside the depicted hand. Afterwards, thresholding using Otsu's method [14] is applied in order to segment the marker from the background of the ROI (Fig. 3e).

The correctness of the segmentation is evaluated based on a plausibility check using the shape of the segmented object. First and second moments of the segmented object are used to determine its position and orientation, respectively. An ellipse is fitted to the segmented object and its eccentricity is used in order to verify if the tube-shaped passive marker has been detected (Fig. 3f).

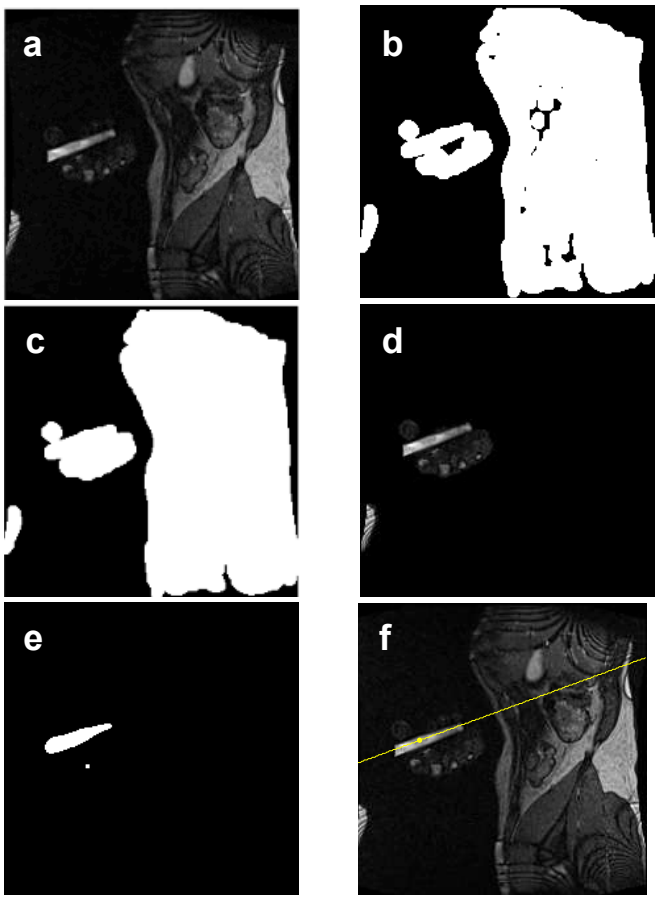

Fig. 3: Detection of position and orientation of the passive marker on a clinical real-time sagittal oblique image.

D. System Architecture

Communication between the MRI HOST PC and an external PC is performed via an Ethernet connection and a proprietary Siemens protocol (ReModProt, Siemens Corporate Research & Technology, USA). The MRI host PC sends the acquired images to the external PC where the images are displayed and image processing and image plane calculations are performed. Afterwards, the commands for position and orientation of the image plane are returned to the MRI HOST for an image plane update. The communication interface on the external PC was implemented in C++ using open source libraries such as Qt, Insight Toolkit (ITK) and Visualization Toolkit (VTK).

E. Precision Assessment

The tracking workflow was repeated 20 times at a given position, as follow: 1 dedicated transversal projection at isocenter for initialization, followed by 3 clinical real-time images (first sagittal, first transversal and second sagittal

Position error [mm]	Sagittal 1	Transversal 1	Sagittal 2
Mean	0.90	0.74	0.73
Standard deviation	0.61	0.55	0.40
Orientation error [°]	Sagittal 1	Transversal 1	Sagittal 2
Mean	0.27	0.25	0.19
Standard deviation	0.17	0.17	0.10

TABLE I: Errors for the image position and orientation, for each of the 3 first real-time images of the workflow.

images) for passive-marker image plane alignment. For each of the 3 clinical real-time image planes, the test device position and orientation are calculated. The mean and standard deviation of the error in position and orientation, respectively, are calculated to assess the test-device tracking precision.

IV. RESULTS

Mean and standard deviation of the error in position and orientation, respectively, are displayed in table I for each of the 3 first clinical real-time image planes of the workflow. Mean position error is on the order of half a real-time clinical image pixel (0.79 ± 0.52 mm), while mean orientation error is $0.24° \pm 0.15°$.

V. DISCUSSION

In this work, a workflow for MR image plane alignment based on detection and tracking in real-time clinical MR images, without any active tracking device, is presented. A test device, an image-based tracking algorithm and a software interface have been developed. First experiments have shown promising results for test-device tracking precision, with a mean position error of 0.79 mm, i.e. about half a pixel in real-time clinical images, and a mean orientation error of 0.24°. The proposed workflow was designed to minimize dedicated acquisition time. In the ideal case, only one dedicated, non-clinically relevant projection image is acquired for the initialization of test device detection. The proposed test device is an original combination of 2 wireless resonant micro-coils and a passive marker. The micro-coils allow for an automated object detection, hence no manual user initialization step is required. Test device tracking is then performed directly in the clinical real-time images through detection of the passive marker. Alternation of axial and sagittal imaging planes allow for a good spatial depiction of the anatomy, necessary for medical procedure. Time for updating a sagittal from an axial image or vice-versa includes acquisition and image reconstruction time as well as time for PC communication protocol and detection algorithm. The current update rate is 1.2 s (axial to sagittal or vice-versa). Further experiments will be carried out for the evaluation of the tracking performance for a given motion of the test device.

VI. ACKNOWLEDGMENT

Authors would like to thank Wilfried Uhring, Daniel Gounot and Pr. Afshin Gangi for their support.

REFERENCES

[1] K. Qing, L. Pan, B. Fetics, F. K. Wacker, S. Valdeig, M. Philip, A. Roth, E. Nevo, D. L. Kraitchman, A. J. v. d. Kouwe, and C. H. Lorenz, "A multi-slice interactive real-time sequence integrated with the EndoScout tracking system for interventional MR guidance," in *Proceedings of the 18th Annual Meeting of ISMRM*, 2010, p. 1860.

[2] S. Alt, A. Homagk, R. Umathum, W. Semmler, and M. Bock, "Active microcoil tracking in the lungs using a semisolid rubber as signal source," *Magnetic Resonance in Medicine*, vol. 64, no. 1, pp. 271–279, 2010. [Online]. Available: http://dx.doi.org/10.1002/mrm.22424

[3] R. Blanco Sequeiros, R. Klemola, R. Ojala, L. Jyrkinen, E. Lappi-Blanco, Y. Soini, and O. Tervonen, "MRI-guided trephine biopsy and fine-needle aspiration in the diagnosis of bone lesions in low-field (0.23 t) MRI system using optical instrument tracking." *European Radiology*, vol. 12, no. 4, pp. 830–835, Apr. 2002.

[4] R. Viard, N. Betrouni, J. Rousseau, S. Mordon, O. Ernst, and S. Maouche, "Needle positioning in interventional MRI procedure: real time optical localisation and accordance with the roadmap," in *Engineering in Medicine and Biology Society, 2007. EMBS 2007. 29th Annual International Conference of the IEEE*, 2007, pp. 2748–2751.

[5] O. Felfoul, J. B. Mathieu, G. Beaudoin, and S. Martel, "In vivo MR-tracking based on magnetic signature selective excitation," *IEEE Transactions on Medical Imaging*, vol. 27, no. 1, pp. 28–35, Jan. 2008, PMID: 18270059. [Online]. Available: http://www.ncbi.nlm.nih.gov/pubmed/18270059

[6] S. P. DiMaio, E. Samset, G. Fischer, I. Iordachita, G. Fichtinger, F. Jolesz, and C. M. Tempany, "Dynamic MRI scan plane control for passive tracking of instruments and devices," in *Proceedings of the 10th international conference on Medical image computing and computer-assisted intervention*, ser. MICCAI'07. Berlin, Heidelberg: Springer-Verlag, 2007, pp. 50–58. [Online]. Available: http://portal.acm.org/citation.cfm?id=1775835.1775843

[7] A. de Oliveira, J. Rauschenberg, D. Beyersdorff, W. Semmler, and M. Bock, "A new system for passive tracking of a prostate biopsy device with automatic 3D needle position estimation," in *Proceedings of the 16th Annual Meeting of ISMRM*, 2008, p. 3003.

[8] F. Maier, A. Krafft, R. Stafford, J. Yung, R. Dillmann, W. Semmler, and M. Bock, "3D passive marker tracking for MR-Guided interventions," in *Proceedings of the 19th Annual Meeting of ISMRM*, 2011, p. 3749.

[9] F. Maier, A. Krafft, R. de Oliveira, W. Semmler, and M. Bock, "MRPen 3D marker tracking for percutaneous interventions," in *Proceedings of the 17th Annual Meeting of ISMRM*, 2009, p. 4421.

[10] M. Rea, D. McRobbie, H. Elhawary, Z. Tse, M. Lamperth, and I. Young, "Sub-pixel localisation of passive micro-coil fiducial markers in interventional MRI," *Magnetic Resonance Materials in Physics, Biology and Medicine*, vol. 22, pp. 71–76, 2009, 10.1007/s10334-008-0143-1. [Online]. Available: http://dx.doi.org/10.1007/s10334-008-0143-1

[11] C. Flask, D. Elgort, E. Wong, A. Shankaranarayanan, J. Lewin, M. Wendt, and J. L. Duerk, "A method for fast 3D tracking using tuned fiducial markers and a limited projection reconstruction FISP (LPR-FISP) sequence," *Journal of Magnetic Resonance Imaging*, vol. 14, no. 5, pp. 617–627, 2001. [Online]. Available: http://dx.doi.org/10.1002/jmri.1227

[12] L. Pan, J. Barbot, S. Shea, S. Patil, K. Kirchberg, G. Meredith, T. Meng, E. Kholmovski, S. Vijayakumar, K. Vij, M. Guttmann, P. Piferi, K. Jenkins, and C. Lorenz, "An integrated system for catheter tracking and visualization in MR-Guided cardiovascular interventions," in *Proceedings of the 19th Annual Meeting of ISMRM*, 2011, p. 195.

[13] A. de Oliveira, J. Rauschenberg, D. Beyersdorff, W. Semmler, and M. Bock, "Automatic passive tracking of an endorectal prostate biopsy device using phase-only cross-correlation," *Magnetic Resonance in Medicine*, vol. 59, no. 5, pp. 1043–1050, 2008. [Online]. Available: http://dx.doi.org/10.1002/mrm.21430

[14] N. Otsu, "A threshold selection method from Gray-Level histograms," *IEEE Transactions on Systems, Man and Cybernetics*, vol. 9, no. 1, pp. 62–66, Jan. 1979.